Perspective

Sound-Absorbing Materials

Sibo Huang,[1,2] Yong Li,[1,*] Jie Zhu,[1,†] and Din Ping Tsai[2,‡]

[1] *Institute of Acoustics, School of Physics Science and Engineering, Tongji University, 200092 Shanghai, China*
[2] *Department of Electrical Engineering, City University of Hong Kong, Hong Kong, China*

(Received 10 April 2023; published 20 July 2023)

Sound-absorbing materials (SAMs) have attracted significant interest for more than a century owing to their rich physical properties and extensive potential in acoustic engineering. This article provides an overview of recent progress in and future prospects for SAMs, from single resonators to coupled resonant systems. Single resonant SAMs use resonances to achieve high-efficiency absorption in a certain bandwidth with a significantly smaller thickness than porous SAMs. The emergence of sound-absorbing metamaterials has led to further thinner structures at deep-subwavelength scales. Coupled resonant systems offer new opportunities for broadband sound absorption and multifunctionality. We introduce the conservation equations for single resonators and general SAMs, outlining the design strategies for achieving tunable and broadband SAMs approaching the optimal conditions governed by the conservation equations. We also review recent developments in multifunctional SAMs and metaliners. Finally, we provide an outlook on potential directions and applications for future work in this rapidly evolving field.

DOI: 10.1103/PhysRevApplied.20.010501

I. INTRODUCTION

Sound-absorbing materials (SAMs) are designed to dissipate sound energy via the thermal-viscous effect near the structure-medium interfaces [1–4]. The design of SAMs involves numerous important considerations, including absorption efficiency, working bandwidth, structural thickness, structural weight, manufacturing complexity, and other mechanical and material properties. These factors should be carefully designed to meet the specific requirements of a given application. Over the years, the research field of SAMs has produced a wealth of excellent results for efficient sound absorption under diverse conditions. Various porous SAMs have been proposed with increased sound-absorbing efficiency, durability, flame resistivity, and human safety [3–7] [Figs. 1(a) and 1(b)].

In addition, numerous resonant SAMs, such as panel absorbers [8,9], microperforated-panel (MPP) absorbers [10,11], and their combination with porous materials [12,13], have resulted in abundant effective designs for medium-frequency to low-frequency absorption and broadband absorption [Figs. 1(c) and 1(f)]. Furthermore, the emergence and development of sound-absorbing metamaterials (SAMMs) in recent years [14–17] have offered new avenues for the development of SAMs. SAMMs are artificially structured materials of subwavelength thickness that provide high-efficiency and/or tunable sound-absorption performance. These metamaterial-based sound absorbers [18–21] offer further increased tunability in acoustic properties over conventional SAMs, leading to fascinating and versatile results.

In this paper, we provide an overview of recent developments in and future prospects for SAMs, from single resonators to coupled resonant systems. We begin by introducing the fundamental principles of sound absorption and the conservation quality of single resonant SAMs, followed by discussions of the recent relevant research in this field. We then focus on coupled resonant SAMs, which use the coupling of multiple resonators to achieve tunable, high-efficiency, and broadband absorption. We introduce the causality principle that governs the conservation quality of general SAMs and outline the design strategies for broadband SAMs approaching the causality-governed optimal thickness. Furthermore, we discuss multifunctional SAMs and the application potentials of SAMMs in environments with airflow. Finally, we conclude by offering perspectives on potential future directions for the development and application of SAMs.

II. SINGLE RESONANT SAMS

A. Theoretical models for sound absorption based on acoustic impedance and coupled-mode theory

Acoustic impedance is a critical parameter for characterizing and designing SAMs. On the basis of the normal

*yongli@tongji.edu.cn
†jiezhu@tongji.edu.cn
‡dptsai@cityu.edu.hk

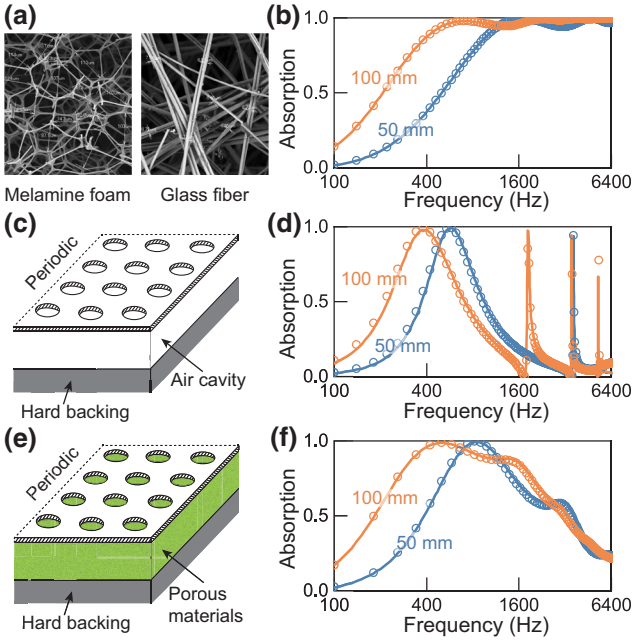

FIG. 1. Conventional SAMs. (a) The microstructures of melamine foam and glass fiber. (b) Theoretical (lines) and simulation (circles; conducted with COMSOL MULTIPHYSISCS) absorption curves of the porous SAMs with thicknesses of 50 mm (in blue) and 100 mm (in orange). The flow resistance (χ_p) of the porous materials is 10 000 Pa s/m^2. (c) An MPP absorber. (d) The absorption curves of the MPP absorbers with overall thicknesses (the sums of the MPP thicknesses and the cavity depths) of 50 mm (in blue) and 100 mm (in orange). The cavity depths (l_c) are 49 mm (in blue) and 99 mm (in orange), respectively. The hole diameter (d_m), panel thickness (t_m), and perforated ratio (σ_m) of the MPPs are 0.5 mm, 1 mm, and 1%, respectively. (e) An MPP absorber combined with porous SAMs. (f) The absorption curves of two MPP absorbers combined with porous SAMs. The overall thicknesses of the two MPP absorbers are 50 mm (in blue) and 100 mm (in orange), respectively. $d_m = 0.8$ mm, $t_m = 1$ mm, $\sigma_m = 2.56\%$, $\chi_p = 10\,000$, and $l_c = 49$ mm (in blue) or $l_c = 99$ mm (in orange). The thicknesses of the porous materials are 49 mm (in blue) and 99 mm (in orange), filling the air cavities of the two MPP absorbers. (a) Reprinted with permission from Ref. [7].

specific acoustic impedance (Z_s), the reflection coefficients of SAMs at normal incidence can be expressed as

$$r = \frac{Z_s - Z_0}{Z_s + Z_0}, \tag{1}$$

where $Z_0 = \rho_0 c_0$, with Z_0, ρ_0, and c_0 being the characteristic acoustic impedance of, static density of, and sound speed of the surrounding medium, respectively. The absorption coefficients can then be calculated by $\alpha = 1 - |r|^2$. Coupled-mode theory [22–26] can also serve as a fundamental tool for describing resonant SAMs. On the basis of coupled-mode theory, the reflection coefficients (r) of a resonator in a one-port system can be expressed as

$$r = 1 - \frac{2Q_{\text{rad}}^{-1}}{2i(\omega/\omega_r - 1) + Q_{\text{rad}}^{-1} + Q_{\text{loss}}^{-1}}, \tag{2}$$

where ω is the angular frequency, ω_r is the angular resonant frequency, and Q_{rad}^{-1} and Q_{loss}^{-1} represent the radiation and intrinsic-loss factors, respectively. $Q_{\text{rad}}^{-1} = 2\gamma/\omega_r$ and $Q_{\text{loss}}^{-1} = 2\Gamma/\omega_r$, with γ and Γ being the radiative and dissipative decay rates. The quality factor (Q) of a resonator can be calculated as $Q^{-1} = Q_{\text{rad}}^{-1} + Q_{\text{loss}}^{-1}$. Equation (2) can be equally written as $r = 1 - (2\gamma/i(\omega - \omega_r) + \gamma + \Gamma)$. The interaction between γ and Γ determines the absorption coefficients, and the "critical coupling" condition ($\gamma = \Gamma$) [23,27–30] leads to perfect absorption [Fig. 2(a)].

This implies that significant intrinsic loss is not the essential requirement for high-efficiency absorption. Recent studies demonstrate that one can achieve ultranarrowband perfect absorption with extremely-low-dissipation resonators by construction of a quasibound state in the continuum (quasiBIC) that supports tunable and extremely low radiation [25,35,36].

B. Conservation equation for single resonant SAMs

The acoustic impedance and resonant frequency of a single resonant SAM can be expressed, respectively, as $Z_s = R_s + i(\omega M_s - K_s/\omega)$ and $\omega_r = \sqrt{K_{sr}/M_{sr}}$, where R_s, M_s, and K_s, respectively, represent the acoustic resistance, mass, and stiffness, and R_{sr}, M_{sr}, and K_{sr} indicate their values at resonance. By substituting the expressions for Z_s and ω_r into Eqs. (1) and (2) and considering the definition $Q_{\text{loss}}^{-1} = R_{sr}/\omega_r M_{sr}$, we can derive $Q_{\text{rad}}^{-1} = Z_0/\omega_r M_{sr}$, where Z_0 and R_{sr} are related to the radiation loss and intrinsic loss of the resonance, respectively. These equations lead to the single-resonator conservation equation as

$$\frac{1}{Qf_r} = \frac{2\pi(Z_0 + R_{sr})}{K_{sr}}, \tag{3}$$

where f_r is the resonant frequency. With Eq. (3), we can deduce the conservation qualities of various specific single resonant SAMs. For example, the acoustic reactance of the Helmholtz resonator shown in Fig. 2(b) is $-i\rho_0 c_0 \cot(k_0 l_c) s_A/s_c$, whose series expansion can be written as $-i\rho_0 c_0 (1/k_0 l_c - k_0 l_c/3 - (k_0 l_c)^3/45 - o(k_0 l_c)^4) s_A/s_c$. The terms after the first term are characterized as acoustic mass, and then K_{sr} is $\rho_0 c_0^2 s_A/s_c l_c$. By substituting this into Eq. (3), we obtain the conservation equation for Helmholtz resonators: $1/Qf_r = 2\pi(1 + R_{sr}/Z_0) s_c l_c/s_A c_0$. Similarly, the conservation equation for the curled-space resonator shown in Fig. 2(c) is $1/Qf_r = (2\pi(1 + R_{sr}/Z_0) s_c l_c/s_A c_0)((s_c + b) s_a/s_c(s_a + b))$. Assuming that the neck of the Helmholtz resonator is embedded

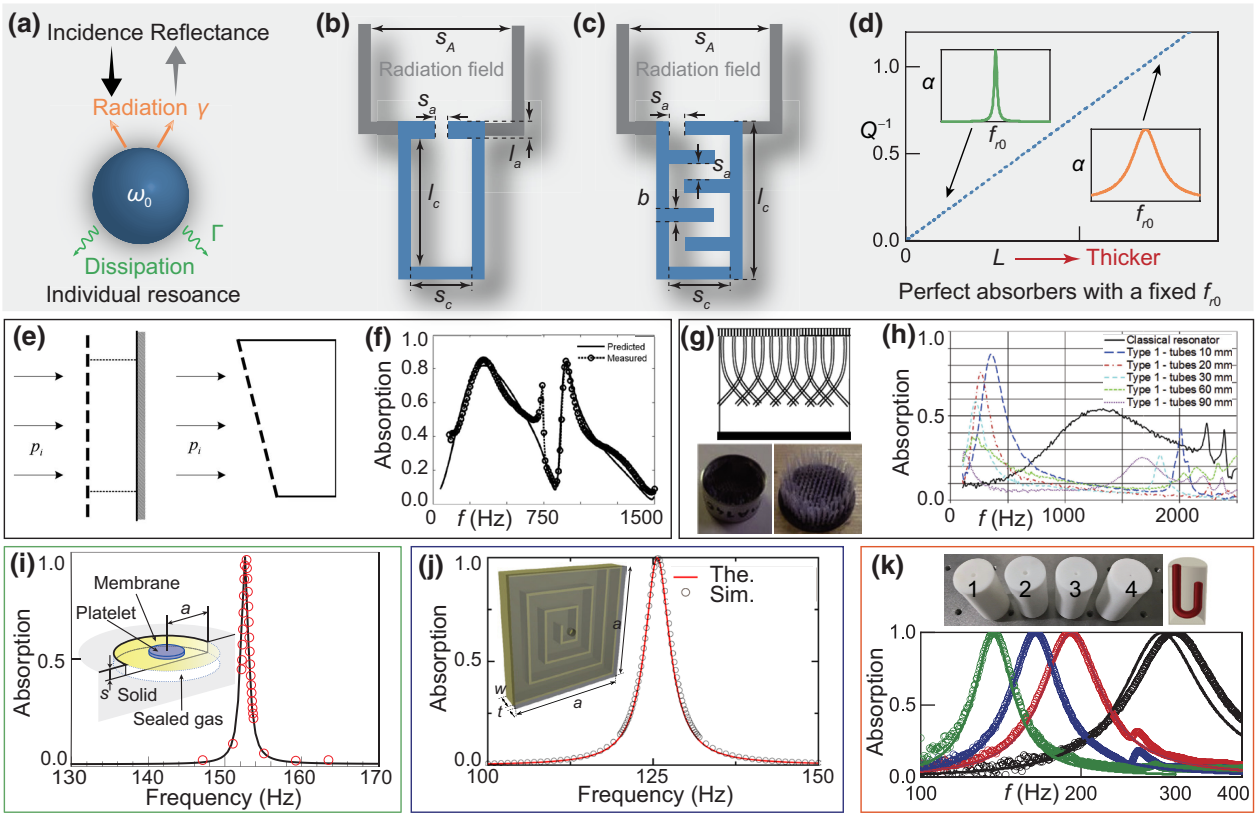

FIG. 2. Single resonant SAMs. (a) A resonant mode. (b) A Helmholtz resonator and (c) a curled-space resonator. (d) Conceptional demonstration of the conservation quality of single resonant perfect SAMs with a fixed resonance frequency f_{r0}. (e) Normal and irregularly shaped MPP absorbers. (f) Absorption curves of an irregularly shaped MPP absorber. (g),(h) Schematic and pictures of MPP absorbers with embedded elastic long necks and their absorption curves with different neck lengths. (i) Absorption curves of a membrane-type absorber. (j) Absorption curves of a curled-space absorber. (k) Absorption curves of four NEHRs having the same shape. Sim., simulation; The., theory. (e),(f) Reprinted with permission from Ref. [11]. (g),(h) Reprinted with permission from Ref. [31]. (i) Reprinted with permission from Ref. [32]. (j) Reprinted with permission from Ref. [33]. (k) Reprinted with permission from Ref. [34].

[34] and the wall thickness is infinitely thin, Helmholtz resonators and curled-space resonators both lead to

$$\frac{1}{Qf_r} = \frac{2\pi(1+R_{sr}/Z_0)L}{c_0}\frac{s_c}{s_A}, \tag{4}$$

where L is the thickness of the overall SAMs. This equation provides the conservation quality of single resonant SAMs regarding their absorption bandwidths (Q), absorption peaks (referring to R_{sr}), resonance frequencies (f_r), and structural thicknesses (L), as exemplified in Fig. 2(d). In addition, Eq. (4) can be further revised by considering the thermal-viscous effect in the air cavities.

Furthermore, understanding the optimal conditions for SAMs is of great importance, and we discuss this on the basis of the conservation quality. By combining Eqs. (1) and (4), we can obtain

$$\frac{1}{Qf_r} = \frac{4\pi L}{c_0}\frac{s_c}{s_A}\frac{1}{1+\sqrt{1-\alpha_r}} \quad (\text{for } R_{sr} < Z_0), \tag{5}$$

$$\frac{1}{Qf_r} = \frac{4\pi L}{c_0}\frac{s_c}{s_A}\frac{1}{1-\sqrt{1-\alpha_r}} \quad (\text{for } R_{sr} \geq Z_0), \tag{6}$$

where α_r is the absorption coefficient at resonance. Equations (5) and (6) demonstrate that when $R_{sr} < Z_0$ (underdamped), it is possible to increase the absorption efficiency, reduce the thickness, and reduce the resonant frequency simultaneously. However, when $R_{sr} \geq Z_0$ (overdamped), the improvements of these three aspects become contradictory. Therefore, excluding the evaluation of wall thickness, we can regard a single resonant SAM reaching the overdamped condition as an optimal design.

C. Deep-subwavelength and tunable single resonant SAMs

Equation (4) indicates that SAMs can achieve perfect absorption with a very thin structure, but their working bandwidths decrease with decreasing ratio of thickness and resonant wavelength, as illustrated in Fig. 2(d). Conventional single resonant SAMs such as MPP absorbers and

their modified designs [11,31] [Figs. 2(e) and 1(h)] can generally achieve high-efficiency absorption in moderate bandwidths with a thickness on the order of a few tenths of the resonant wavelength (λ_r) [10–12,37–40]. In recent years, SAMMs, such as membrane-type SAMMs [32,41–45] and curled-space SAMMs [33,46–53], have pushed the performance limit in some scenarios. For example, a membrane-type absorber composed of a mass-plate-decorated membrane and an air cavity achieved perfect absorption at 152 Hz with a thickness of 17.2 mm ($\lambda_r/131$) [32] [Fig. 2(i)]. A curled-space absorber exhibited perfect absorption with a thickness of $\lambda_r/223$ [33] [Fig. 2(j)]. A multicoiled absorber realized perfect absorption at 50 Hz with a thickness of only 13 mm ($\lambda_r/523$) [52]. For those deep-subwavelength SAMMs, as predicted by Eq. (4), their working bandwidths are proportional to L/λ_r.

Recent progress in SAMMs has demonstrated that high tunability is crucial for achieving target absorption under various restrictions [34,51,53–61]. In the design of highly tunable SAMMs, the conservation equation can serve as an effective tool to evaluate absorption performance. For instance, neck-embedded Helmholtz resonators (NEHRs) offered free modulation of working frequencies and bandwidths under a constant shape [34,54] [Fig. 2(k)]. Neck-embedded curled channels realized tunable working bandwidths under a constant resonant frequency [51] or tunable working frequencies under a constant shape [53]. Curled channels with unequal sections exhibited tunable working frequencies and bandwidths [55,62,63]. Despite the abundant variations in absorption performances arising from high tunability, we can theoretically predict the absorption potentials of these tunable SAMMs.

III. COUPLED RESONANT SAMS

A. Theoretical models for coupled resonant SAMs and the causality constraint

The coupling effect among acoustic resonators can be analyzed through impedance analysis. When the cross sections of coupled resonant SAMs are of subwavelength scales where the fundamental-mode reflection is dominant, their overall acoustic impedance ($Z_{\rm cs}$) can be expressed as

$$Z_{\rm cs} = 1/\sum_{n=1}^{N}(Z_{{\rm is}(n)}^{-1}), \tag{7}$$

where $Z_{{\rm is}(n)}$ represents the surface impedance of the nth-component resonator and N is the total number of coupled resonators. Additionally, acoustic grating theory [64] can be applied when the higher-order waves cannot be ignored.

Temporal coupled-mode theory provides another effective pathway to investigate the coupling among multiple resonant modes [Fig. 3(a)], where the nth mode ($\tilde{a}_{(n)} = a_{(n)}e^{i\omega t}$) can be expressed as [25,68–70]

$$\frac{d}{dt}\tilde{a}_{(n)} = (i\omega_{r(n)} - \gamma_{(n)} - \Gamma_{(n)})\tilde{a}_{(n)} + i\sqrt{\gamma_{(n)}}\tilde{S}_i^{+} + \sum_{m\neq n}\left(\left(-\sqrt{\gamma_{(n)}}\sqrt{\gamma_{(m)}}\Lambda_{nm} + i\kappa_{nm}\right)\tilde{a}_{(m)}\right), \tag{8}$$

where $\tilde{S}_i^{+} = S_i^{+}e^{i\omega t}$ represents the incident waves, and κ_{nm} and $-\sqrt{\gamma_{(n)}}\sqrt{\gamma_{(m)}}\Lambda_{nm}$, respectively, denote the near-field and far-field coupling factors between the nth mode and the mth mode [69]. The reflection coefficient of the coupled resonant system can then be calculated by

$$r = 1 + 2i\sum_{n=1}^{N}\left(\sqrt{\gamma_{(n)}}\frac{a_{(n)}}{S_i^{+}}\right), \tag{9}$$

where N is the total number of coupled modes. On the basis of Eq. (9), we can further calculate the overall acoustic impedance by $Z_{\rm cs} = (1+r)/(1-r)$.

For linear and passive SAMs with an acoustically rigid backing, the causality equation is obtained by accumulating dissipation on the lower-half complex wavelength plane [Fig. 3(b)], which leads to [67]

$$L \geq = \frac{1}{4\pi^2\phi}\left|\int_0^{\infty}\ln|1 - A(\lambda)|\,d\lambda\right| = L_{\rm min}, \tag{10}$$

where ϕ is the volume fraction of the material, $A(\lambda)$ is the absorption coefficient at wavelength λ, and $L_{\rm min}$ is the causality-governed minimal thickness. Equation (10) demonstrates the conservation quality of a general SAM with respect to its thickness and absorption coefficients over frequencies. Relevant studies have shown that the overdamped condition is necessary for approaching the causality-governed minimal thickness [61,64,71]. By comparing the calculated thicknesses of numerous overdamped single resonant SAMs based on Eqs. (4) and (10), we find that the results are numerically approximate. However, we do not obtain a direct mathematical transformation of Eqs. (4) and (10), which can be attributed to the different fundamental formulas for the thickness-impedance relations used in the derivations of these two equations. In addition, it is noteworthy that the causal constraint can be circumvented by removing the hard-backing condition, such as by using an open-hole backing [72] or a soft-material backing [73,74].

B. Coupled resonant SAMs

The coupling among resonances provides additional degrees of tunability for developing SAMs. By modulating the coupling effect appropriately, we can realize efficient overall absorption performance of a coupled SAM [49,52,75–85] [Fig. 3(c)]. For example, by use of cascading coupling (components arranged in a cascading manner)

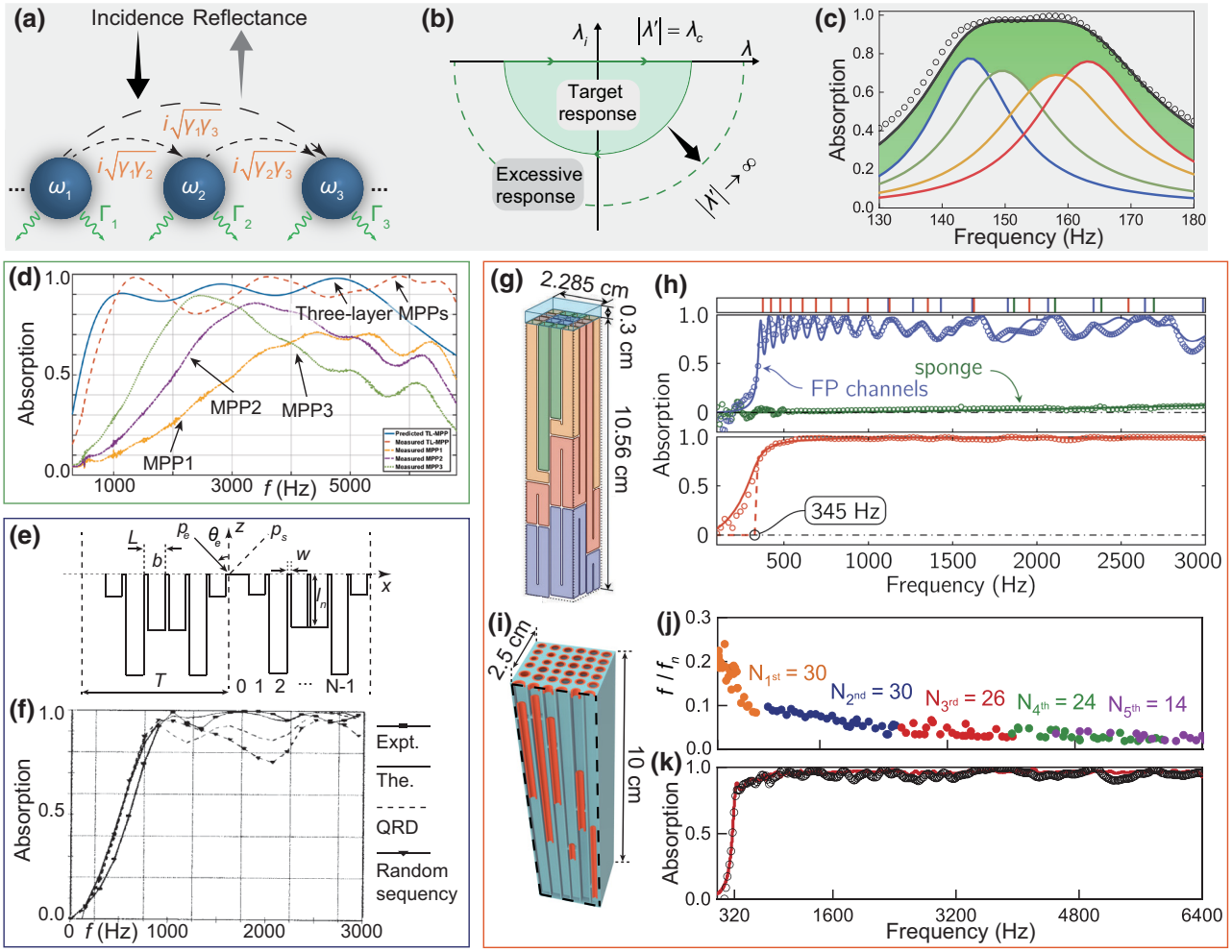

FIG. 3. Coupled resonant SAMMs. (a) Coupling effect among multiple resonant modes. (b) Responses of SAMs in the complex wavelength plane. (c) Use of the coupling effect to modulate the overall absorption performance of a SAMM. (d) Absorption curves of a three-layer MPP absorber. (e) A quadratic residue diffuser (QRD). (f) Absorption curves of the QRD covered with a metal mesh. (g) Coupled resonant absorber consisting of 16 curled channels. (h) Absorption curves of the absorber in (g) (in blue), a 3-mm sponge (in green), and the absorber covered with the sponge (in red). (i) Coupled resonant absorber consisting of 36 cascading NEHRs. (j) The component absorbers support intensive mode density. (k) Absorption curves of the absorber in (i). Expt., experiment; FP, Fabry-Perot; TL, three-layer; The., theory. (b),(i)–(k) Reprinted with permission from Ref. [61]. (c) Reprinted with permission from Ref. [60]. (d) Reprinted with permission from Ref. [65]. (e),(f) Reprinted with permission from Ref. [66]. (g),(h) Reprinted with permission from Ref. [67].

[65,86–90] [Fig. 3(d)] and/or parallel coupling (components arranged in a parallel manner) [66,91–94] [Figs. 3(e) and 3(f)] among multiple traditional resonators, the coupled resonant system can achieve excellent absorption within bandwidths much wider than those of single resonant SAMs. Further increasing the tunability of coupled resonant systems can lead to more broadband absorption and/or more-compact structures than conventional designs. Recent studies have proposed two effective strategies for constructing compact ultrabroadband coupled resonant SAMMs. The first strategy primarily uses the individual absorption of the component absorbers to achieve overall broadband quasiperfect absorption of the coupled resonant systems [49,67]. In this strategy, the individual components commonly exhibit narrowband quasiperfect absorption. The second strategy primarily exploits the coupling effect among component absorbers, where the individual component absorbers commonly deviate from perfect absorption to achieve higher tunability of the coupling effect [60,61,95,96].

Figures 3(g) and 3(h) illustrate a broadband coupled resonant SAMM that approaches the minimum thickness [67]. This absorber follows the first design strategy, where the overall absorption primarily results from the individual absorption of the 16 curled channels with quasiperfect absorption. Further, an additional porous material can be used to increase the mode density and achieve the overdamped condition, thereby effectively increasing

the overall absorption. Figures 3(i) and 3(j) illustrate another broadband coupled resonant absorber approaching the minimum thickness [61]. This absorber follows the second design strategy, where the overall absorption is dominated by the coupling effect among the 36 cascading NEHRs, which individually show imperfect absorption in the overdamped domain. The intensive mode density supported by the 36 cascading NEHRs effectively suppresses the absorption dips at antiresonances, providing a relatively flat absorption curve. The interaction among component resonators in radiation fields can be regarded as far-field coupling. In addition, recent research demonstrates that use of a bridge structure connecting resonators to introduce near-field coupling can improve the coupling modulation of the coupled resonant SAMM, leading to high-efficiency broadband absorption [84]. Furthermore, the design strategies for airborne SAMs may inspire the development of underwater SAMs. In underwater scenarios, a variety of resonant components can be used, including solid cores with soft-viscoelastic-material coatings [97–100], controlled air bubbles [101,102], composite viscoelastic slabs [103,104], rubber-coated Helmholtz resonators [105], composite-material Fabry-Perot resonators [106], and combinations of viscoelastic rubbers, conical cavities, cylindrical oscillators, and backing steels [107]. By suitable modulation of the coupling among these underwater resonant components, a promising avenue can be explored to achieve broadband and efficient underwater sound absorption.

IV. MULTIFUNCTIONAL SAMS AND METALINERS

A. Multifunctional SAMs

The progress made in coupled resonant SAMs provides new techniques and strategies for effectively modulating absorption-related properties, which paves the way for the development of multifunctional SAMs [61,96,108–112]. For example, SAMM-based acoustic barriers have demonstrated remarkable potential for achieving both outstanding ventilation and broadband sound insulation [113–118], as shown in Fig. 4(a).

Through the design methods that focus on wave interference, such as band-structure analysis [121–124] and effective-medium theory [125,126], strong sound-reflective ventilated structures with a wide frequency range have been achieved. Furthermore, SAMMs enable acoustic barriers with ventilation to effectively utilize the combined effects of sound absorption and reflection. This allows the further widening of the operating range by incorporation of absorption-dominated, absorption-reflection coaction, and reflection-dominated frequency bands [113]. A compact multifunctional metastructure composed of multiple NEHRs with a hexagonal honeycomb configuration realized both low-frequency broadband sound absorption and excellent crash-energy dissipation [96], as shown in Figs. 4(b) and 4(c). A recently proposed metasilencer achieves delicate modulation of mode density and intrinsic loss, which enables versatile sound control, including alleviation, highlighting, and muting of different overtones for broadband, leading to a designable timbre [108], as shown in Fig. 4(d). An acoustic quasiBIC-supporting system composed of two coupled low-dissipation cavities with a small length difference can achieve high Q as well as tunable perfect absorption and strong acoustic-pressure-field enhancement [25], as shown in Figs. 4(e) and 4(f).

B. Metaliners

Acoustic liners are widely used in aircraft engines and exhaust mufflers to reduce noise levels [127,128]. Although many conventional designs can effectively reduce noise for target modes in relatively narrow bands [129–131], challenges such as broadband sound attenuation, deep-subwavelength thickness, and high tolerance to varying flow speeds still remain. Recently, SAMMs have shown great potential in addressing these challenges [64,119,120,132–136]. Figure 4(g) illustrates a metaliner based on SAMMs [119]. The NEHR array of the metaliner contributes to the thinness, the desired impedance condition in broadband, and the more-unconstrained design of the front perforated panel that leads to increased tolerance to speed-varying flows [Figs. 4(h) and 4(i)]. Another metaliner composed of multiple neck-embedded curled channels exhibits higher sound-attenuation efficiency as well as a wider working bandwidth than a traditional double-degree-of-freedom liner under airflow [120] [Figs. 4(j) and 4(k)]. However, efforts are still needed to develop efficient acoustic metaliners capable of handling higher-intensity sound, higher flow speeds, and more-complicated sound-propagating modes.

V. OUTLOOK

Recent advancements in SAMs have made it possible to achieve high-efficiency, deep-subwavelength, broadband, and tunable designs. Besides, the conservation equations of SAMs now allow us to predict their potential theoretically. Despite the significant progress made in this field, we can envision numerous exciting opportunities and promising directions for the future development and application of SAMs.

One area that requires attention is ultrabroadband SAMMs based on coupled resonant structures. Their complex configurations make them difficult to manufacture. Researchers can explore advanced manufacturing techniques and new design concepts for ultrabroadband SAMMs to address this issue. For example, new designs of tunable single resonant SAMs that are easier to assemble may lead to less-complicated coupled resonant structures. The combination of SAMMs and traditional SAMs, such

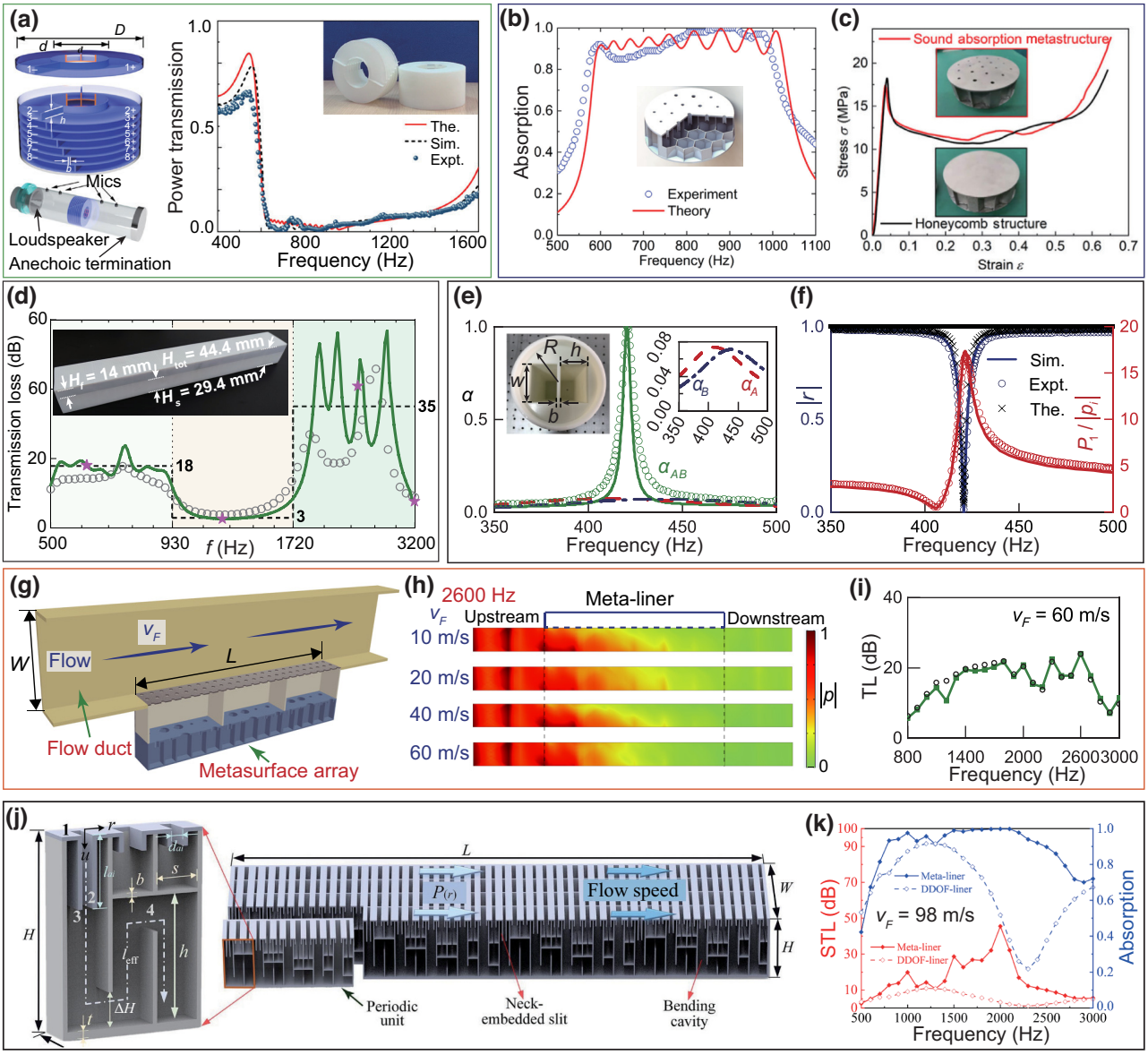

FIG. 4. Multifunctional SAMs and metaliners. (a) Acoustic power transmission of an acoustic barrier with ventilation. (b) Absorption curves of a multifunctional metastructure. (c) Stress-strain curves of the multifunctional metastructure and a honeycomb structure under quasistatic uniaxial compression. (d) Transmission-loss curves of a metasilencer with a designable timbre. (e) Absorption curves of a two-cavity coupled system (green) and the two individual cavities (in blue and red, respectively). (f) Reflection factor (blue) of the two-cavity coupled system and the pressure amplification (red) at the bottom center of the cavity. (g) Cut-open view of a side-branched metaliner with NEHRs in a flow duct. (h) Distributions of sound-pressure amplitudes of the metaliner under various speeds of grazing flow. (i) Transmission-loss (TL) curves of the metaliner under a grazing flow of 60 m/s. (j) A metaliner with neck-embedded curled channels. (k) Comparison of the sound transmission loss (STL) between the metaliner (solid line) and a DDOF liner (dotted line) under a grazing flow of 98 m/s. Expt., experiment; Mics, microphones, Sim., simulation; The., theory; (a) Reprinted with permission from Ref. [113]. (b),(c) Reprinted with permission from Ref. [96]. (d) Reprinted with permission from Ref. [108]. (f) Reprinted with permission from Ref. [25]. (g)–(i) Reprinted with permission from Ref. [119]. (j),(k) Reprinted with permission from Ref. [120].

as metaporous [137–141] and modified MPP absorbers [60,64,142,143], may offer a desired trade-off between performance and structure complexity.

Recent studies have shown that acoustic soft boundaries in SAMs can achieve novel absorption performance that cannot be realized by SAMs with acoustically hard backings [72–74]. Further exploration in this direction shows promise for innovative SAMs. In addition, recent studies have demonstrated that coupled resonant SAMMs with both near-field and far-field couplings [84,124] can bring additional freedom to modulate the coupling effect and lead to efficient designs. Considering that most of

the previously proposed coupled resonant SAMMs rely on the far-field coupling to modulate absorption performance, we can expect fruitful new results in future exploration in this direction. Furthermore, new designs for SAMs are being inspired by acoustic black holes [144–149], origami structures [150–153], microstructural designs [154–157], etc.

Multifunctional SAMs have been the subject of increasing research attention, and future efforts should explore the richer multifunctionality of SAMMs. For example, tunable broadband SAMs could benefit many acoustic functional devices in impedance engineering by modulating acoustic reflection and radiation in the broadband range [158,159]. Ultranarrowband (high-Q) absorption recently observed in quasiBIC-supporting systems may provide an application platform for high-sensitivity sensing and filtering [25,35]. Besides, recent studies have demonstrated that the enhancement of pressure fields of acoustic resonant structures can facilitate acoustic energy harvesting [160–162], which is another significant research direction for quasiBIC-supporting SAMs. Furthermore, researchers may investigate the mechanical properties, material properties, and interactions with application environments in addition to sound absorption to explore multifunctional SAMs.

High-intensity sound and airflow are two factors that weaken the absorption performance of SAMs in real applications. Recent studies have shown that SAMM-based metaliners can mitigate the impact of the two factors. Future research may explore how to utilize these seemingly negative factors to improve the performance of SAMMs in real applications.

Advanced algorithms such as deep learning have been shown to be efficient tools for designing SAMs with on-demand performances [85,163–165]. Future research in this area holds great promise. In addition, introducing active controls to SAMs will provide new techniques to design acoustic properties with reduced size and weight [166–169], which is another future direction highly worth exploring.

Overall, new ideas continue to emerge in the field of SAMs, leading to more-powerful and more-versatile designs for a wider range of application platforms. Thus, we conclude that the future of SAMs is promising.

ACKNOWLEDGMENTS

This work was supported by the National Natural Science Foundation of China under Grant No. 12074286, the Shanghai Science and Technology Committee under Grant No. 21JC1405600, and the University Grants Committee of the Research Grants Council of the Hong Kong Special Administrative Region, China, under Grant No. AoE/P-502/20.

[1] U. Ingard, On the theory and design of acoustic resonators, J. Acoust. Soc. Am. **25**, 1037 (1953).
[2] M. R. Stinson, The propagation of plane sound waves in narrow and wide circular tubes, and generalization to uniform tubes of arbitrary cross-sectional shape, J. Acoust. Soc. Am. **89**, 550 (1991).
[3] M. Delany and E. Bazley, Acoustical properties of fibrous absorbent materials, Appl. Acoust. **3**, 105 (1970).
[4] J.-F. Allard and Y. Champoux, New empirical equations for sound propagation in rigid frame fibrous materials, J. Acoust. Soc. Am. **91**, 3346 (1992).
[5] L. Cao, Q. Fu, Y. Si, B. Ding, and J. Yu, Porous materials for sound absorption, Compos. Commun. **10**, 25 (2018).
[6] N. Kino and T. Ueno, Comparisons between characteristic lengths and fibre equivalent diameters in glass fibre and melamine foam materials of similar flow resistivity, Appl. Acoust. **69**, 325 (2008).
[7] N. Kino, Further investigations of empirical improvements to the Johnson–Champoux–Allard model, Appl. Acoust. **96**, 153 (2015).
[8] M. Toyoda, K. Sakagami, D. Takahashi, and M. Morimoto, Effect of a honeycomb on the sound absorption characteristics of panel-type absorbers, Appl. Acoust. **72**, 943 (2011).
[9] M. Arunkumar, M. Jagadeesh, J. Pitchaimani, K. Gangadharan, and M. L. Babu, Sound radiation and transmission loss characteristics of a honeycomb sandwich panel with composite facings: Effect of inherent material damping, J. Sound Vib. **383**, 221 (2016).
[10] D.-Y. Maa, Potential of microperforated panel absorber, J. Acoust. Soc. Am. **104**, 2861 (1998).
[11] C. Wang, L. Cheng, J. Pan, and G. Yu, Sound absorption of a micro-perforated panel backed by an irregular-shaped cavity, J. Acoust. Soc. Am. **127**, 238 (2010).
[12] Z. Liu, J. Zhan, M. Fard, and J. L. Davy, Acoustic properties of multilayer sound absorbers with a 3D printed micro-perforated panel, Appl. Acoust. **121**, 25 (2017).
[13] M. Toyoda, K. Sakagami, M. Okano, T. Okuzono, and E. Toyoda, Improved sound absorption performance of three-dimensional MPP space sound absorbers by filling with porous materials, Appl. Acoust. **116**, 311 (2017).
[14] M. Yang and P. Sheng, Sound absorption structures: From porous media to acoustic metamaterials, Annu. Rev. Mater. Res. **47**, 83 (2017).
[15] S. Qu and P. Sheng, Microwave and Acoustic Absorption Metamaterials, Phys. Rev. Appl. **17**, 047001 (2022).
[16] N. Gao, Z. Zhang, J. Deng, X. Guo, B. Cheng, and H. Hou, Acoustic metamaterials for noise reduction: A review, Adv. Mater. Technol. **7**, 2100698 (2022).
[17] X. Zhang, Z. Qu, and H. Wang, Engineering acoustic metamaterials for sound absorption: From uniform to gradient structures, Iscience **23**, 101110 (2020).
[18] G. Ma and P. Sheng, Acoustic metamaterials: From local resonances to broad horizons, Sci. Adv. **2**, e1501595 (2016).
[19] S. A. Cummer, J. Christensen, and A. Alù, Controlling sound with acoustic metamaterials, Nat. Rev. Mater. **1**, 1 (2016).
[20] B. Assouar, B. Liang, Y. Wu, Y. Li, J.-C. Cheng, and Y. Jing, Acoustic metasurfaces, Nat. Rev. Mater. **3**, 460 (2018).

[21] J. Li, X. Wen, and P. Sheng, Acoustic metamaterials, J. Appl. Phys. **129**, 171103 (2021).
[22] S. H. Fan, W. Suh, and J. D. Joannopoulos, Temporal coupled-mode theory for the Fano resonance in optical resonators, J. Opt. Soc. Am. A **20**, 569 (2003).
[23] Y. Xu, Y. Li, R. K. Lee, and A. Yariv, Scattering-theory analysis of waveguide-resonator coupling, Phys. Rev. E **62**, 7389 (2000).
[24] C. Qu, S. Ma, J. Hao, M. Qiu, X. Li, S. Xiao, Z. Miao, N. Dai, Q. He, S. Sun, *et al.*, Tailor the Functionalities of Metasurfaces Based on a Complete Phase Diagram, Phys. Rev. Lett. **115**, 235503 (2015).
[25] S. Huang, T. Liu, Z. Zhou, X. Wang, J. Zhu, and Y. Li, Extreme Sound Confinement from Quasibound States in the Continuum, Phys. Rev. Appl. **14**, 021001 (2020).
[26] H. Long, C. Liu, C. Shao, Y. Cheng, J. Tao, X. Qiu, and X. Liu, Tunable and broadband asymmetric sound absorptions with coupling of acoustic bright and dark modes, J. Sound Vib. **479**, 115371 (2020).
[27] K. Y. Bliokh, Y. P. Bliokh, V. Freilikher, S. Savel'ev, and F. Nori, Colloquium: Unusual resonators: Plasmonics, metamaterials, and random media, Rev. Mod. Phys. **80**, 1201 (2008).
[28] N. Jiménez, W. Huang, V. Romero-García, V. Pagneux, and J. P. Groby, Ultra-thin metamaterial for perfect and quasi-omnidirectional sound absorption, Appl. Phys. Lett. **109**, 121902 (2016).
[29] V. Romero-García, G. Theocharis, O. Richoux, A. Merkel, V. Tournat, and V. Pagneux, Perfect and broadband acoustic absorption by critically coupled sub-wavelength resonators, Sci. Rep. **6**, 1 (2016).
[30] H. Long, Y. Cheng, J. Tao, and X. Liu, Perfect absorption of low-frequency sound waves by critically coupled subwavelength resonant system, Appl. Phys. Lett. **110**, 023502 (2017).
[31] F. Simon, Long elastic open neck acoustic resonator for low frequency absorption, J. Sound Vib. **421**, 1 (2018).
[32] G. Ma, M. Yang, S. Xiao, Z. Yang, and P. Sheng, Acoustic metasurface with hybrid resonances, Nat. Mater. **13**, 873 (2014).
[33] Y. Li and B. M. Assouar, Acoustic metasurface-based perfect absorber with deep subwavelength thickness, Appl. Phys. Lett. **108**, 063502 (2016).
[34] S. Huang, X. Fang, X. Wang, B. Assouar, Q. Cheng, and Y. Li, Acoustic perfect absorbers via Helmholtz resonators with embedded apertures, J. Acoust. Soc. Am. **145**, 254 (2019).
[35] L. Huang, Y. Chiang, S. Huang, C. Shen, F. Deng, Y. Cheng, B. Jia, Y. Li, D. A. Powell, and A. E. Miroshnichenko, Sound trapping in an open resonator, Nat. Commun. **12**, 4819 (2021).
[36] L. Huang, B. Jia, Y. K. Chiang, S. Huang, C. Shen, F. Deng, T. Yang, D. A. Powell, Y. Li, and A. E. Miroshnichenko, Topological supercavity resonances in the finite system, Adv. Sci. **9** (2022), 2200257.
[37] J. Ning, S. Ren, and G. Zhao, Acoustic properties of micro-perforated panel absorber having arbitrary cross-sectional perforations, Appl. Acoust. **111**, 135 (2016).
[38] S. Huang, S. Li, X. Wang, and D. Mao, Micro-perforated absorbers with incompletely partitioned cavities, Appl. Acoust. **126**, 114 (2017).
[39] J. Carbajo, J. Ramis, L. Godinho, and P. Amado-Mendes, Perforated panel absorbers with micro-perforated partitions, Appl. Acoust. **149**, 108 (2019).
[40] J. Shen, H. P. Lee, and X. Yan, Sound absorption performance and mechanism of flexible PVA microperforated membrane, Appl. Acoust. **185**, 108420 (2022).
[41] J. Mei, G. Ma, M. Yang, Z. Yang, W. Wen, and P. Sheng, Dark acoustic metamaterials as super absorbers for low-frequency sound, Nat. Commun. **3**, 756 (2012).
[42] M. Yang, C. Meng, C. Fu, Y. Li, Z. Yang, and P. Sheng, Subwavelength total acoustic absorption with degenerate resonators, Appl. Phys. Lett. **107**, 104104 (2015).
[43] C. Fu, X. Zhang, M. Yang, S. Xiao, and Z. Yang, Hybrid membrane resonators for multiple frequency asymmetric absorption and reflection in large waveguide, Appl. Phys. Lett. **110**, 021901 (2017).
[44] T. Xing, X. Gai, J. Zhao, X. Li, Z. Cai, X. Guan, and F. Wang, Low frequency sound absorption of adjustable membrane-type acoustic metamaterials, Appl. Acoust. **188**, 108586 (2022).
[45] Q. Xu, J. Qiao, Z. Ren, J. Sun, G. Zhang, and L. Li, Multi synergistic coupling design for broadband sound absorption based on compact porous composite embedded with massless membrane resonator, Compos. Struct. **286**, 115312 (2022).
[46] Z. Liang and J. Li, Extreme Acoustic Metamaterial by Coiling up Space, Phys. Rev. Lett. **108**, 114301 (2012).
[47] Y. Li, B. Liang, X. Tao, X. F. Zhu, X. Y. Zou, and J. C. Cheng, Acoustic focusing by coiling up space, Appl. Phys. Lett. **101**, 233508 (2012).
[48] X. B. Cai, Q. Q. Guo, G. K. Hu, and J. Yang, Ultrathin low-frequency sound absorbing panels based on coplanar spiral tubes or coplanar Helmholtz resonators, Appl. Phys. Lett. **105**, 121901 (2014).
[49] C. Zhang and X. Hu, Three-Dimensional Single-Port Labyrinthine Acoustic Metamaterial: Perfect Absorption with Large Bandwidth and Tunability, Phys. Rev. Appl. **6**, 064025 (2016).
[50] L. Liu, H. Chang, C. Zhang, and X. Hu, Single-channel labyrinthine metasurfaces as perfect sound absorbers with tunable bandwidth, Appl. Phys. Lett. **111**, 083503 (2017).
[51] S. Huang, X. Fang, X. Wang, B. Assouar, Q. Cheng, and Y. Li, Acoustic perfect absorbers via spiral metasurfaces with embedded apertures, Appl. Phys. Lett. **113**, 233501 (2018).
[52] K. Donda, Y. Zhu, S.-W. Fan, L. Cao, Y. Li, and B. Assouar, Extreme low-frequency ultrathin acoustic absorbing metasurface, Appl. Phys. Lett. **115**, 173506 (2019).
[53] J. Guo, X. Zhang, Y. Fang, and R. Qu, An extremely-thin acoustic metasurface for low-frequency sound attenuation with a tunable absorption bandwidth, Int. J. Mech. Sci. **213**, 106872 (2022).
[54] J. Guo, X. Zhang, Y. Fang, and Z. Jiang, A compact low-frequency sound-absorbing metasurface constructed by resonator with embedded spiral neck, Appl. Phys. Lett. **117**, 221902 (2020).
[55] Y. Wang, H. Zhao, H. Yang, J. Zhong, D. Zhao, Z. Lu, and J. Wen, A tunable sound-absorbing metamaterial based on coiled-up space, J. Appl. Phys. **123**, 185109 (2018).

[56] D. Kong, S. Huang, D. Li, C. Cai, Z. Zhou, B. Liu, G. Cao, X. Chen, Y. Li, and S. Liu, Low-frequency multi-order acoustic absorber based on spiral metasurface, J. Acoust. Soc. Am. **150**, 12 (2021).
[57] D. Li, S. Huang, Y. Cheng, and Y. Li, Compact asymmetric sound absorber at the exceptional point, Sci. China–Phys. Mech. Astron. **64**, 244303 (2021).
[58] Q. Xu, J. Qiao, J. Sun, G. Zhang, and L. Li, A tunable massless membrane metamaterial for perfect and low-frequency sound absorption, J. Sound Vib. **493**, 115823 (2021).
[59] C. Song, S. Huang, Z. Zhou, J. Zhang, B. Jia, C. Zhou, Y. Li, and Y. Pan, Perfect acoustic absorption of Helmholtz resonators via tapered necks, Appl. Phys. Express **15**, 084006 (2022).
[60] S. Huang, Z. Zhou, D. Li, T. Liu, X. Wang, J. Zhu, and Y. Li, Compact broadband acoustic sink with coherently coupled weak resonances, Sci. Bull. **65**, 373 (2020).
[61] Z. Zhou, S. Huang, D. Li, J. Zhu, and Y. Li, Broadband impedance modulation via non-local acoustic metamaterials, Natl. Sci. Rev. **9**, nwab171 (2022).
[62] Y. Wang, H. Zhao, H. Yang, J. Zhong, and J. Wen, A space-coiled acoustic metamaterial with tunable low-frequency sound absorption, Europhys. Lett. **120**, 54001 (2018).
[63] Y. Han, X. Wang, G. Xie, X. Tang, and T. Chen, Low-frequency sound-absorbing metasurface with a channel of nonuniform cross section, J. Appl. Phys. **127**, 064902 (2020).
[64] H. Ding, N. Wang, S. Qiu, S. Huang, Z. Zhou, C. Zhou, B. Jia, and Y. Li, Broadband acoustic meta-liner with metal foam approaching causality-governed minimal thickness, Int. J. Mech. Sci. **232**, 107601 (2022).
[65] P. Cobo, C. de la Colina, E. Roibas-Millan, M. Chimeno, and F. Simon, A wideband triple-layer microperforated panel sound absorber, Compos. Struct. **226**, 111226 (2019).
[66] T. Wu, T. J. Cox, and Y. W. Lam, From a profiled diffuser to an optimized absorber, J. Acoust. Soc. Am. **108**, 643 (2000).
[67] M. Yang, S. Chen, C. Fu, and P. Sheng, Optimal sound-absorbing structures, Mater. Horiz. **4**, 673 (2017).
[68] W. Tan, Y. Sun, Z. G. Wang, and H. Chen, Manipulating electromagnetic responses of metal wires at the deep subwavelength scale via both near- and far-field couplings, Appl. Phys. Lett. **104**, 091107 (2014).
[69] W. Zhu, X. Fang, D. Li, Y. Sun, Y. Li, Y. Jing, and H. Chen, Simultaneous Observation of a Topological Edge State and Exceptional Point in an Open and Non-Hermitian Acoustic System, Phys. Rev. Lett. **121**, 124501 (2018).
[70] S. Huang, S. Xie, H. Gao, T. Hao, S. Zhang, T. Liu, Y. Li, and J. Zhu, Acoustic Purcell effect induced by quasibound state in the continuum, *Fundam. Res.* (to be published).
[71] C. Shao, Y. Zhu, H. Long, C. Liu, Y. Cheng, and X. Liu, Metasurface absorber for ultra-broadband sound via overdamped modes coupling, Appl. Phys. Lett. **120**, 083504 (2022).
[72] H. Y. Mak, X. Zhang, Z. Dong, S. Miura, T. Iwata, and P. Sheng, Going Beyond the Causal Limit in Acoustic Absorption, Phys. Rev. Appl. **16**, 044062 (2021).
[73] S. Cui and R. L. Harne, Soft Materials with Broadband and Near-Total Absorption of Sound, Phys. Rev. Appl. **12**, 064059 (2019).
[74] N. Gao, S. Qu, J. Li, J. Wang, and W. Chen, Harnessing post-buckling deformation to tune sound absorption in soft Helmholtz absorbers, Int. J. Mech. Sci. **208**, 106695 (2021).
[75] J. Li, W. Wang, Y. Xie, B.-I. Popa, and S. A. Cummer, A sound absorbing metasurface with coupled resonators, Appl. Phys. Lett. **109**, 091908 (2016).
[76] X. Jiang, B. Liang, R.-q. Li, X.-y. Zou, L.-l. Yin, and J.-c. Cheng, Ultra-broadband absorption by acoustic metamaterials, Appl. Phys. Lett. **105**, 243505 (2014).
[77] N. Jiménez, V. Romero-García, V. Pagneux, and J. P. Groby, Rainbow-trapping absorbers: Broadband, perfect and asymmetric sound absorption by subwavelength panels for transmission problems, Sci. Rep. **7**, 13595 (2017).
[78] Y. Qian, J. Zhang, N. Sun, D. Kong, and X. Zhang, Pilot study on wideband sound absorber obtained by adopting a serial-parallel coupling manner, Appl. Acoust. **124**, 48 (2017).
[79] X. Peng, J. Ji, and Y. Jing, Composite honeycomb metasurface panel for broadband sound absorption, J. Acoust. Soc. Am. **144**, EL255 (2018).
[80] H. Long, C. Shao, C. Liu, Y. Cheng, and X. Liu, Broadband near-perfect absorption of low-frequency sound by subwavelength metasurface, Appl. Phys. Lett. **115**, 103503 (2019).
[81] Y. Zhu, K. Donda, S. Fan, L. Cao, and B. Assouar, Broadband ultra-thin acoustic metasurface absorber with coiled structure, Appl. Phys. Express **12**, 114002 (2019).
[82] N. Gao, D. Luo, B. Cheng, and H. Hou, Teaching-learning-based optimization of a composite metastructure in the 0–10 kHz broadband sound absorption range, J. Acoust. Soc. Am. **148**, EL125 (2020).
[83] C. R. Liu, J. H. Wu, Z. Yang, and F. Ma, Ultra-broadband acoustic absorption of a thin microperforated panel metamaterial with multi-order resonance, Compos. Struct. **246**, 112366 (2020).
[84] Y. Zhu, A. Merkel, K. Donda, S. Fan, L. Cao, and B. Assouar, Nonlocal acoustic metasurface for ultrabroadband sound absorption, Phys. Rev. B **103**, 064102 (2021).
[85] L. Liu, L.-X. Xie, W. Huang, X. J. Zhang, M.-H. Lu, and Y.-F. Chen, Broadband acoustic absorbing metamaterial via deep learning approach, Appl. Phys. Lett. **120**, 251701 (2022).
[86] S.-H. Park, Acoustic properties of micro-perforated panel absorbers backed by Helmholtz resonators for the improvement of low-frequency sound absorption, J. Sound Vib. **332**, 4895 (2013).
[87] T. Bravo, C. Maury, and C. Pinhède, Enhancing sound absorption and transmission through flexible multi-layer micro-perforated structures, J. Acoust. Soc. Am. **134**, 3663 (2013).
[88] X.-D. Zhao, Y.-J. Yu, and Y.-J. Wu, Improving low-frequency sound absorption of micro-perforated panel absorbers by using mechanical impedance plate combined with Helmholtz resonators, Appl. Acoust. **114**, 92 (2016).
[89] H.-S. Kim, P.-S. Ma, S.-R. Kim, S.-H. Lee, and Y.-H. Seo, A model for the sound absorption coefficient of

multi-layered elastic micro-perforated plates, J. Sound Vib. **430**, 75 (2018).
[90] X. Yang, P. Bai, X. Shen, S. To, L. Chen, X. Zhang, and Q. Yin, Optimal design and experimental validation of sound absorbing multilayer microperforated panel with constraint conditions, Appl. Acoust. **146**, 334 (2019).
[91] T. Wu, T. J. Cox, and Y. Lam, A profiled structure with improved low frequency absorption, J. Acoust. Soc. Am. **110**, 3064 (2001).
[92] C. Wang and L. Huang, On the acoustic properties of parallel arrangement of multiple micro-perforated panel absorbers with different cavity depths, J. Acoust. Soc. Am. **130**, 208 (2011).
[93] C. Wang, L. Huang, and Y. Zhang, Oblique incidence sound absorption of parallel arrangement of multiple micro-perforated panel absorbers in a periodic pattern, J. Sound Vib. **333**, 6828 (2014).
[94] D. Li, D. Chang, and B. Liu, Enhancing the low frequency sound absorption of a perforated panel by parallel-arranged extended tubes, Appl. Acoust. **102**, 126 (2016).
[95] V. Rajendran, A. Piacsek, and T. Méndez Echenagucia, Design of broadband Helmholtz resonator arrays using the radiation impedance method, J. Acoust. Soc. Am. **151**, 457 (2022).
[96] Z. Ren, Y. Cheng, M. Chen, X. Yuan, and D. Fang, A compact multifunctional metastructure for low-frequency broadband sound absorption and crash energy dissipation, Mater. Des. **215**, 110462 (2022).
[97] J. Wen, H. Zhao, L. Lv, B. Yuan, G. Wang, and X. Wen, Effects of locally resonant modes on underwater sound absorption in viscoelastic materials, J. Acoust. Soc. Am. **130**, 1201 (2011).
[98] T. Brunet, J. Leng, and O. Mondain-Monval, Soft acoustic metamaterials, Science **342**, 323 (2013).
[99] Y. Zhang and L. Cheng, Ultra-thin and broadband low-frequency underwater acoustic meta-absorber, Int. J. Mech. Sci. **210**, 106732 (2021).
[100] B. Liu, S. Huang, B. Zheng, X. Chen, J. Zhao, X. Qi, Y. Li, and S. Liu, Tunable composite lattice structure for low-frequency and ultra-broadband underwater sound absorption, J. Acoust. Soc. Am. **153**, 415 (2023).
[101] Y. Fu, J. Fischer, K. Pan, G. H. Yeoh, and Z. Peng, Underwater sound absorption properties of polydimethylsiloxane/carbon nanotube composites with steel plate backing, Appl. Acoust. **171**, 107668 (2021).
[102] T. Wang, G.-B. Wang, R.-J. Zhang, and M.-Z. Ke, Low-frequency underwater sound absorption metamaterial, Phys. Scr. **97**, 125706 (2022).
[103] H. Meng, J. Wen, H. Zhao, and X. Wen, Optimization of locally resonant acoustic metamaterials on underwater sound absorption characteristics, J. Sound Vib. **331**, 4406 (2012).
[104] H. Zhao, J. Wen, H. Yang, L. Lv, and X. Wen, Backing effects on the underwater acoustic absorption of a viscoelastic slab with locally resonant scatterers, Appl. Acoust. **76**, 48 (2014).
[105] M. Duan, C. Yu, F. Xin, and T. J. Lu, Tunable underwater acoustic metamaterials via quasi-Helmholtz resonance: From low-frequency to ultra-broadband, Appl. Phys. Lett. **118**, 071904 (2021).
[106] S. Qu, N. Gao, A. Tinel, B. Morvan, V. Romero-García, J.-P. Groby, and P. Sheng, Underwater metamaterial absorber with impedance-matched composite, Sci. Adv. **8**, eabm4206 (2022).
[107] N. Gao and K. Lu, An underwater metamaterial for broadband acoustic absorption at low frequency, Appl. Acoust. **169**, 107500 (2020).
[108] N. Wang, C. Zhou, S. Qiu, S. Huang, B. Jia, S. Liu, J. Cao, Z. Zhou, H. Ding, J. Zhu, *et al.*, Meta-silencer with designable timbre, Int. J. Extreme Manuf. **5**, 025501 (2023).
[109] B. Lu, L. Lv, H. Yang, J. Gao, T. Xu, G. Sun, X. Jin, C. Shao, L. Qu, and J. Yang, High performance broadband acoustic absorption and sound sensing of a bubbled graphene monolith, J. Mater. Chem. A **7**, 11423 (2019).
[110] Y. Zhu and B. Assouar, Multifunctional acoustic metasurface based on an array of Helmholtz resonators, Phys. Rev. B **99**, 174109 (2019).
[111] Y. Jin, Y. Yang, Z. Wen, L. He, Y. Cang, B. Yang, B. Djafari-Rouhani, Y. Li, and Y. Li, Lightweight sound-absorbing metastructures with perforated fish-belly panels, Int. J. Mech. Sci. **226**, 107396 (2022).
[112] X. Li, X. Yu, M. Zhao, Z. Li, Z. Wang, and W. Zhai, Multilevel bioinspired microlattice with broadband sound-absorption capabilities and deformation-tolerant compressive response, Adv. Funct. Mater. **33**, 2210160 (2023).
[113] R. Dong, D. Mao, X. Wang, and Y. Li, Ultrabroadband Acoustic Ventilation Barriers via Hybrid-Functional Metasurfaces, Phys. Rev. Appl. **15**, 024044 (2021).
[114] R. Dong, M. Sun, F. Mo, D. Mao, X. Wang, and Y. Li, Recent advances in acoustic ventilation barriers, J. Phys. D **54**, 403002 (2021).
[115] T. Lee, T. Nomura, E. M. Dede, and H. Iizuka, Ultrasparse Acoustic Absorbers Enabling Fluid Flow and Visible-Light Controls, Phys. Rev. Appl. **11**, 024022 (2019).
[116] X. Xiang, X. Wu, X. Li, P. Wu, H. He, Q. Mu, S. Wang, Y. Huang, and W. Wen, Ultra-open ventilated metamaterial absorbers for sound-silencing applications in environment with free air flows, Extreme Mech. Lett. **39**, 100786 (2020).
[117] S. Kumar and H. P. Lee, Labyrinthine acoustic metastructures enabling broadband sound absorption and ventilation, Appl. Phys. Lett. **116**, 134103 (2020).
[118] X. Xiang, H. Tian, Y. Huang, X. Wu, and W. Wen, Manually tunable ventilated metamaterial absorbers, Appl. Phys. Lett. **118**, 053504 (2021).
[119] S. Huang, E. Zhou, Z. Huang, P. Lei, Z. Zhou, and Y. Li, Broadband sound attenuation by metaliner under grazing flow, Appl. Phys. Lett. **118**, 063504 (2021).
[120] J. Zhao, F. Wu, Z.-G. Ju, M. Hu, X. Zhang, D. Li, S.-L. Yan, and K.-L. Liu, Neck-embedded acoustic meta-liner for the broadband sound-absorbing under the grazing flow with a wide speed range, J. Phys. D **56**, 045401 (2022).
[121] Z.-x. Xu, H. Gao, Y.-j. Ding, J. Yang, B. Liang, and J.-c. Cheng, Topology-Optimized Omnidirectional Broadband Acoustic Ventilation Barrier, Phys. Rev. Appl. **14**, 054016 (2020).
[122] C. Liu, H. Wang, B. Liang, J.-c. Cheng, and Y. Lai, Low-frequency and broadband muffler via cascaded

labyrinthine metasurfaces, Appl. Phys. Lett. **120**, 231702 (2022).
[123] X. Cui, C. Liu, J. Shi, C. Shen, X. Liu, and Y. Lai, A flexible meta-curtain for simultaneous soundproofing and ventilation, Symmetry **14**, 2348 (2022).
[124] Y. Zhu, R. Dong, D. Mao, X. Wang, and Y. Li, Nonlocal Ventilating Metasurfaces, Phys. Rev. Appl. **19**, 014067 (2023).
[125] M. Sun, X. Fang, D. Mao, X. Wang, and Y. Li, Broadband Acoustic Ventilation Barriers, Phys. Rev. Appl. **13**, 044028 (2020).
[126] C. Liu, J. Shi, W. Zhao, X. Zhou, C. Ma, R. Peng, M. Wang, Z. H. Hang, X. Liu, J. Christensen, *et al.*, Three-Dimensional Soundproof Acoustic Metacage, Phys. Rev. Lett. **127**, 084301 (2021).
[127] X. Ma and Z. Su, Development of acoustic liner in aero engine: A review, Sci. China Technol. Sci. **63**, 2491 (2020).
[128] C. Lahiri and F. Bake, A review of bias flow liners for acoustic damping in gas turbine combustors, J. Sound Vib. **400**, 564 (2017).
[129] J. D. Eldredge and A. P. Dowling, The absorption of axial acoustic waves by a perforated liner with bias flow, J. Fluid Mech. **485**, 307 (2003).
[130] X. Qiu, B. Xin, L. Wu, Y. Meng, and X. Jing, Investigation of straightforward impedance eduction method on single-degree-of-freedom acoustic liners, Chin. J. Aeronaut. **31**, 2221 (2018).
[131] X. Zhang and L. Cheng, Acoustic impedance of micro-perforated panels in a grazing flow, J. Acoust. Soc. Am. **145**, 2461 (2019).
[132] J. Guo, Y. Fang, Z. Jiang, and X. Zhang, An investigation on noise attenuation by acoustic liner constructed by Helmholtz resonators with extended necks, J. Acoust. Soc. Am. **149**, 70 (2021).
[133] L. Shen, Y. Zhu, F. Mao, S. Gao, Z. Su, Z. Luo, H. Zhang, and B. Assouar, Broadband Low-Frequency Acoustic Metamuffler, Phys. Rev. Appl. **16**, 064057 (2021).
[134] T. S. Oh and W. Jeon, Acoustic metaliners for sound insulation in a duct with little flow resistance, Appl. Phys. Lett. **120**, 044103 (2022).
[135] F. Wu, Z. Ju, Z. Geng, J. Zhao, M. Hu, G. She, H. Pu, J. Luo, and P. Xiang, Low frequency and broadband sound attenuation by meta-liner under grazing flow and high sound intensity, AIP Adv. **12**, 085109 (2022).
[136] J. Guo, R. Qu, Y. Fang, W. Yi, and X. Zhang, A phase-gradient acoustic metasurface for broadband duct noise attenuation in the presence of flow, Int. J. Mech. Sci. **237**, 107822 (2023).
[137] C. Lagarrigue, J.-P. Groby, V. Tournat, O. Dazel, and O. Umnova, Absorption of sound by porous layers with embedded periodic arrays of resonant inclusions, J. Acoust. Soc. Am. **134**, 4670 (2013).
[138] J.-P. Groby, C. Lagarrigue, B. Brouard, O. Dazel, V. Tournat, and B. Nennig, Enhancing the absorption properties of acoustic porous plates by periodically embedding Helmholtz resonators, J. Acoust. Soc. Am. **137**, 273 (2015).
[139] T. G. Zieliński, K. C. Opiela, P. Pawłowski, N. Dauchez, T. Boutin, J. Kennedy, D. Trimble, H. Rice, B. Van Damme, G. Hannema, *et al.*, Reproducibility of sound-absorbing periodic porous materials using additive manufacturing technologies: Round robin study, Addit. Manuf. **36**, 101564 (2020).
[140] N. Gao, J. Wu, K. Lu, and H. Zhong, Hybrid composite meta-porous structure for improving and broadening sound absorption, Mech. Syst. Signal Process. **154**, 107504 (2021).
[141] F. Ma, C. Wang, Y. Du, Z. Zhu, and J. H. Wu, Enhancing of broadband sound absorption through soft matter, Mater. Horiz. **9**, 653 (2022).
[142] D. Li, S. Huang, F. Mo, X. Wang, and y. Li, Low-frequency broadband absorbers based on coupling micro-perforated panel and space-curling chamber, Chi. Sci. Bull. **65**, 1420 (2020).
[143] F. Wu, Y. Xiao, D. Yu, H. Zhao, Y. Wang, and J. Wen, Low-frequency sound absorption of hybrid absorber based on micro-perforated panel and coiled-up channels, Appl. Phys. Lett. **114**, 151901 (2019).
[144] A. Pelat, F. Gautier, S. C. Conlon, and F. Semperlotti, The acoustic black hole: A review of theory and applications, J. Sound Vib. **476**, 115316 (2020).
[145] X. Zhang and L. Cheng, Broadband and low frequency sound absorption by sonic black holes with micro-perforated boundaries, J. Sound Vib. **512**, 116401 (2021).
[146] Y. Mi, L. Cheng, W. Zhai, and X. Yu, Broadband low-frequency sound attenuation in duct with embedded periodic sonic black holes, J. Sound Vib. **536**, 117138 (2022).
[147] J. W. Chua, X. Li, X. Yu, and W. Zhai, Novel slow-sound lattice absorbers based on the sonic black hole, Compos. Struct. **304**, 116434 (2023).
[148] O. Umnova, D. Brooke, P. Leclaire, and T. Dupont, Multiple resonances in lossy acoustic black holes-theory and experiment, J. Sound Vib. **543**, 117377 (2023).
[149] T. Bravo and C. y. Maur, Broadband sound attenuation and absorption by duct silencers based on the acoustic black hole effect: Simulations and experiments, J. Sound Vib. **561**, 117825 (2023).
[150] T. Cambonie and E. Gourdon, Innovative origami-based solutions for enhanced quarter-wavelength resonators, J. Sound Vib. **434**, 379 (2018).
[151] X. Yu, H. Fang, F. Cui, L. Cheng, and Z. Lu, Origami-inspired foldable sound barrier designs, J. Sound Vib. **442**, 514 (2019).
[152] P. Jiang, T. Jiang, and Q. He, Origami-based adjustable sound-absorbing metamaterial, Smart Mater. Struct. **30**, 057002 (2021).
[153] G. Wen, S. Zhang, H. Wang, Z.-P. Wang, J. He, Z. Chen, J. Liu, and Y. M. Xie, Origami-based acoustic metamaterial for tunable and broadband sound attenuation, Int. J. Mech. Sci. **239**, 107872 (2023).
[154] K. C. Opiela and T. G. Zieliński, Microstructural design, manufacturing and dual-scale modelling of an adaptable porous composite sound absorber, Compos. B: Eng. **187**, 107833 (2020).
[155] X. Li, X. Yu, and W. Zhai, additively manufactured deformation-recoverable and broadband sound-absorbing microlattice inspired by the concept of traditional perforated panels, Adv. Mater. **33**, 2104552 (2021).

[156] W. Sun, B. Pan, X. Song, H. Xiao, J. Zhou, and D. Sui, A novel sound absorber design of nanofibrous composite porous material, Mater. Des. **214**, 110418 (2022).

[157] K. Pang, X. Liu, J. Pang, A. Samy, J. Xie, Y. Liu, L. Peng, Z. Xu, and C. Gao, Highly efficient cellular acoustic absorber of graphene ultrathin drums, Adv. Mater. **34**, 2103740 (2022).

[158] L. Quan, X. Zhong, X. Liu, X. Gong, and P. A. Johnson, Effective impedance boundary optimization and its contribution to dipole radiation and radiation pattern control, Nat. Commun. **5**, 3188 (2014).

[159] L. Quan and A. Alù, Hyperbolic Sound Propagation over Nonlocal Acoustic Metasurfaces, Phys. Rev. Lett. **123**, 244303 (2019).

[160] K. Ma, T. Tan, Z. Yan, F. Liu, W.-H. Liao, and W. Zhang, Metamaterial and Helmholtz coupled resonator for high-density acoustic energy harvesting, Nano Energy **82**, 105693 (2021).

[161] H. Zhao, X. Xiao, P. Xu, T. Zhao, L. Song, X. Pan, J. Mi, M. Xu, and Z. L. Wang, Dual-tube Helmholtz resonator-based triboelectric nanogenerator for highly efficient harvesting of acoustic energy, Adv. Energy Mater. **9**, 1902824 (2019).

[162] S. Qi, M. Oudich, Y. Li, and B. Assouar, Acoustic energy harvesting based on a planar acoustic metamaterial, Appl. Phys. Lett. **108**, 263501 (2016).

[163] K. Donda, Y. Zhu, A. Merkel, S.-W. Fan, L. Cao, S. Wan, and B. Assouar, Ultrathin acoustic absorbing metasurface based on deep learning approach, Smart Mater. Struct. **30**, 085003 (2021).

[164] A. Chen, Z.-X. Xu, B. Zheng, J. Yang, B. Liang, and J.-C. Cheng, Machine learning-assisted low-frequency and broadband sound absorber with coherently coupled weak resonances, Appl. Phys. Lett. **120**, 033501 (2022).

[165] Z.-x. Xu, B. Zheng, J. Yang, B. Liang, and J.-c. Cheng, Machine-Learning-Assisted Acoustic Consecutive Fano Resonances: Application to a Tunable Broadband Low-Frequency Metasilencer, Phys. Rev. Appl. **16**, 044020 (2021).

[166] Z. Lu, M. Shrestha, and G.-K. Lau, Electrically tunable and broader-band sound absorption by using micro-perforated dielectric elastomer actuator, Appl. Phys. Lett. **110**, 182901 (2017).

[167] B.-I. Popa, Y. Zhai, and H.-S. Kwon, Broadband sound barriers with bianisotropic metasurfaces, Nat. Commun. **9**, 5299 (2018).

[168] C. Shen and S. A. Cummer, Harnessing Multiple Internal Reflections to Design Highly Absorptive Acoustic Metasurfaces, Phys. Rev. Appl. **9**, 054009 (2018).

[169] X. Liu, C. Wang, Y. Zhang, and L. Huang, Investigation of broadband sound absorption of smart micro-perforated panel (MPP) absorber, Int. J. Mech. Sci. **199**, 106426 (2021).